Lawrence Berkeley National Laboratory
Lawrence Berkeley National Laboratory

Title

High resolution x-ray lensless imaging by differential holographic encoding

Permalink

https://escholarship.org/uc/item/0r6527z4

Author

Zhu, D.

Publication Date

2010-03-05

Peer reviewed

High Resolution X-ray Lensless Imaging by Differential Holographic Encoding

Diling Zhu,[1,2] Manuel Guizar-Sicairos,[3] Benny Wu,[1,2] Andreas Scherz,[2]

Yves Acremann,[4] Tolek Tylisczcak,[5] Peter Fischer,[6] Nina Friedenberger,[7]

Katharina Ollefs,[7] Michael Farle,[7] James R. Fienup,[3] Joachim Stöhr[8]

[1]*Department of Applied Physics, Stanford University, Stanford, California, U.S.A.*

[2]*Stanford Institute for Material and Energy Science,*

SLAC National Accelerator Laboratory, Menlo Park, California, U.S.A.

[3]*The Institute of Optics, University of Rochester, Rochester, New York, U.S.A.*

[4]*PULSE Center for Energy Science, SLAC National*

Accelerator Laboratory, Menlo Park, California, U.S.A.

[5]*Chemical Sciences Division, Advanced Light Source,*

Lawrance Berkeley National Laboratory, Berkeley, California, U.S.A.

[6]*Center for X-ray Optics, Lawrance Berkeley National Laboratory, Berkeley, California, U.S.A.*

[7]*Fachbereich Physik and Center for Nanointegration Duisburg-Essen (CeNIDE),*

Universität Duisburg-Essen, Duisburg, Germany.

[8]*Linac Coherent Light Source, SLAC National Accelerator*

Laboratory, Menlo Park, California, U.S.A. and

* Corresponding author: dlzhu@stanford.edu

X-ray free electron lasers (X-FELs) [1, 2] will soon offer femtosecond pulses of laterally coherent x-rays with sufficient intensity to record single-shot coherent scattering patterns for nanoscale imaging [3–6]. Pulse trains created by split-and-delay techniques even open the door for cinematography on unprecedented nanometer length and femtosecond time scales [7, 8]. A key to real space ultrafast motion pictures is fast and reliable inversion of the recorded reciprocal space scattering patterns. Here we for the first time demonstrate in the x-ray regime the power of a novel technique for lensless high resolution imaging, previously suggested by Guizar-Sicairos and Fienup [9] termed holography with

extended reference by autocorrelation linear differential operation, HERALDO. We have achieved superior resolution over conventional x-ray Fourier transform holography (FTH) [10, 11] without sacrifices in SNR or significant increase in algorithmic complexity. By combining images obtained from individual sharp features on an extended reference, we further show that the resolution can be even extended beyond the reference fabrication limits. Direct comparison to iterative phase retrieval image reconstruction and images recorded with state-of-the-art zone plate microscopes is presented. Our results demonstrate the power of HERALDO as a favorable candidate for robust inversion of single-shot coherent scattering patterns.

HERALDO is an off-axis holographic technique in which the reference wave emerges from a sharp feature/edge on an extended structure, and the reconstruction is obtained through differential operations [9, 12]. Unlike previous x-ray lensless holography experiments [11, 13], whose resolution is determined by the size of the small reference features, the resolution of HERALDO is given by the extent of the derivative of the edge response instead, as schematically shown in Fig. 1a,b. The data acquisition and reconstruction process is schematically shown in Figure 1c-f. The recorded coherent scattering data is multiplied by a Fourier domain decoding filter before a final inverse Fourier transform delivers the image. The decoding filter is the Fourier domain equivalent of the differential operator required in object space [14]. This operator is chosen according to the geometry of the reference [9]. As shown in Fig. 1c, the filters for different references share the common feature that they all have smaller values near the center of the diffraction pattern, i.e., the information about the object is preferentially encoded in the higher scattering angles of the diffraction intensity. This renders the method relatively less influenced by the loss of the central part of the diffraction pattern, typically due to overlap with the direct beam or the beamstop shadow and can become an obstacle to achieve high quality reconstructions for previous methods.

We first show that HERALDO can deliver sharper images than FTH, without compromising SNR, using a high contrast "Swiss cheese" pattern as the object. The object and the references are fabricated with a focused ion beam (FIB) on a 200 nm thick gold film supported by a 100 nm thick silicon nitride window. The reference structures chosen in this case are an "L" shaped slit and a small pinhole for comparison with FTH. Because the

pinhole size is highly sensitive to the milling conditions, a series of identical samples were fabricated with varying ion beam doses for the reference pinholes. We chose the sample that has the smallest reference pinhole among the series (~ 40 nm). On the other hand, the width of the "L" shaped slit (~ 20 nm) appears not as sensitive to the variation in ion-beam exposure time, which greatly simplifies the HERALDO reference fabrication. Notice that the slit width determines the resolution in the direction perpendicular to the slit and edge sharpness determines the resolution along the slit.

Reconstructions can be obtained from each end of the L-shaped slit individually by applying a single directional derivative (first order differential operator) along either arm of the "L". This yields two reconstructions with higher resolution than FTH but with reduced SNR due to the narrower slits being weaker references. Although the noise can be reduced by averaging the two reconstructions, for this sample we take an alternative approach that proves to be more robust. Following the general framework in [15], it can be shown that for this reference, upon application of both derivatives (the corresponding Fourier domain filter is shown in Fig. 1e), we obtain three different directional derivatives of the object, which are equivalent to relief images having illumination from different angles, as shown in Fig 2c. This filter corresponds to a second order linear differential operator and provides strong suppression of artifacts caused by missing data. The problem is then reduced to finding an object that can reproduce all of these derivatives, a well-studied problem for wavefront reconstruction from Shack-Hartmann measurements [16–18]. This leads to a reconstruction that is very robust to noise and artifacts, with significant improvement in resolution, while achieving the same level of SNR as FTH. The results are shown in Figure 2d, compared with the FTH reconstruction shown in Figure 2b.

Resolution of HERALDO can be extended beyond reference fabrication limit by combining images obtained from independent sharp features on a single extended reference through a non-iterative computation. We demonstrate this capability by imaging iron/iron oxide nanocube of 18 nm in size [19] using a triangular reference. A closer look at the corners of the triangle reveals a curvature determined by the FIB radius. As a result, each corner scatters photons preferentially along a different direction, sampling the frequency spectrum of the object with high SNR in complimentary regions. We therefore expect the images reconstructed from each corner to have higher resolution along different directions. A composite image of overall higher resolution can be obtained by combining the three images

using a multi-frame Yaroslavsky-Caulfield filter [20], a summation in Fourier space that is weighted by the frequency-dependent SNR of the images. As shown in Fig. 3a, the sample contains nanocubes dispersed on a silicon nitride membrane window with $\sim 50\%$ coverage. The other side of the nitride membrane is coated with a 1 μm thick gold film. A 900 nm $\times$ 900 nm square aperture defines the viewing window. The reference triangle in its vicinity is milled all the way through. Reconstructions from individual corners are combined to yield a significant improvement of the reconstruction resolution beyond the reference fabrication limitation, allowing to clearly resolve single-particle rows and gaps, as shown in Fig. 3c. Resolution determined by line cuts at the edge of different nanocube clusters is 15 ± 1 nm, one example line cut is shown in Fig. 4f.

The HERALDO result provides a good support information for performing an iterative transform algorithm (ITA) [21] on the same coherent scattering pattern. The ITA result is shown in Fig. 4c, with a resolution of 24 nm determined by the line cut (Fig. 4c, f) and the 10-90% criterion. This resolution correspond to the angularly averaged phase retrieval modulation transfer function cut off at 60% [22]. For this experiment, HERALDO achieved higher resolution while ITA was able to better recover the low frequency information that was lost due to the beamstop. Notice that in the outer region of the measured diffraction pattern, where the high resolution information resides, the SNR can be too low for the phase to be consistently recovered by ITA. However, the fringe contrast remains distinguishable, which we believe allows the phase of the object field to be recovered deterministically by holography. There is evidence that with longer exposure ITA can improve on the holographic reconstruction resolution [23], while holography itself works surprisingly well with a small number of scattered photons [24]. However, a general performance comparison between holographic methods and ITA is complicated by the complexity of the reconstruction procedure of the latter and its many algorithmic variations.

We finally compare the HERALDO results with the images obtained with the state-of-the-art zone plate based soft x-ray imaging instruments also at Fe L3 resonance. Fig. 4d is a scanning transmission x-ray microscope (STXM) image obtained at Advanced Light Source (ALS) BL 11.0.2 with a 20 nm focusing zone plate. The scan used 7 nm step size and the total x-ray exposure time is 15 minutes. As expected, the STXM proves to be better at preserving the overall contrast. The image resolution in this case is limited by vibrations, stage and beam intensity drift between each line scan, which one can see from the signature

streaks along the scan direction. Fig. 4e is obtained with the full field transmission x-ray microscope (TXM) XM1 at ALS BL 6.1.2 [25, 26] using a 25 nm zone plate as the high resolution objective lens. Five images of 1.2 second exposures are averaged for the final image. The higher noise level of the TXM image is a consequence of the shorter exposure time. In comparison, while zone plate based methods represent a more general and versatile class of microscopy techniques, HERALDO clearly provides a single shot compatible imaging platform that is capable of delivering superior resolution, and at the same time allows the study of non-repeatable dynamic processes using the X-FEL.

In conclusion, we have demonstrated high-resolution holographic diffractive imaging using HERALDO at x-ray wavelengths. We find the performance of this technique compares well to ITA and zone-plate imaging techniques. We identify HERALDO as a very promising approach for imaging at X-FEL sources because of its compatibility with single shot imaging, its simplified reference fabrication, its fast and simple reconstruction algorithm and its inherent robustness against the missing central part of the data. All parameters relevant to the Fourier decoding filter can be obtained directly from the data, thus no *a priori* quantitative knowledge of the object or reference is needed. We have also found that HERALDO enjoys a higher degree of immunity to noise and artifacts in the data as a benefit of the differential encoding and decoding process. A clever combination of reconstructions from individual sharp features can significantly increase the resolution, sensitivity, and SNR of the reconstructions. Using Coded arrays of similar sharp features as HERALDO references can potentially further improve the imaging efficiency [13]. We envision the implementation of HERALDO to free space imaging of nanoparticles [27] by introducing high-Z nanostructures with sharp edges into the particle beams. These known nanostructures could, in case of coincidental placement, serve as extended references.

I. METHODS

A. Data acquisition

The x-ray diffraction data were recorded at the coherent scattering beamline BL 13-3 at the Stanford Synchrotron Radiation Lightsource. The instrument is described in [28]. For the "cheese" sample, we used a wavelength of 1.9 nm. The beamstop in this case was a $\sim$

1.1 mm diameter epoxy bead supported by a 14 μm thick tungsten wire, blocking a central region of approximately 60 pixels in diameter. For the iron/iron oxide nanocube experiment, we chose the x-ray wavelength at the Fe L3 resonance (708 eV, or 1.76 nm) for elemental contrast. Two data sets with different beamstop sizes ($\sim$ 250 μm and 1.1 mm, 20 minutes total exposure for the latter) were combined to increase the data dynamic range.

B. "Cheese" reconstruction

The application of two directional derivatives allowed us to recover a third reconstruction from the intersection of the two slits. It also helped reduce the artifacts due to the missing data at the beamstop. This third reconstruction further helps in over-constraining the problem and increases the SNR. To alleviate edge effects on the reconstruction, the Fourier domain filter also included some tapering to smooth out the edges of the computational window and the data occluded by the beamstop. Stronger tapering at the beamstop shadow edge was necessary for the FTH reconstruction since this technique is more sensitive to the missing small angle scattering data.

The object was recovered in a robust manner by considering the three obtained relief images as an over-constrained system of linear equations. The problem was then reduced to finding an object that can reproduce all of these derivatives by solving this set of equations, a well-studied problem for wave-front reconstruction. This problem can be solved by a pseudo-inverse but usually iterative methods are preferred as they relax the memory requirements and yield fast and accurate results. For reconstruction we generalized the technique for phase reconstruction for digital shearing laser interferometry in [29] to complex-valued objects. We used a conjugate-gradient nonlinear optimization algorithm to minimize a squared-error metric between the measured derivatives and the derivatives of our current estimate for the object. The gradient of the error metric with respect to the object pixel values was efficiently computed using an analytic expression.

C. Nanocube reconstruction

The diffraction pattern was multiplied by a Fourier filter for reconstruction from each corner. After registering the reconstructions we combined them with a multi-frame Yaroslavsky-

Caulfield filter [20]. Although this filter can be used to deconvolve the PSF associated with each corner, we use the filter only for noise regularization since a good estimate of the PSFs is not available.

D. Iterative phase retrieval

The separated, non-centrosymmetric support is favorable for phase retrieval [30]. For the reconstruction, every 45 hybrid input-output iterations were followed by 5 iterations of error reduction [21], with 1000 iterations in total. The best result was obtained using an expanding weighting function on the measured data, as described in [30, 31]. The algorithm was allowed to freely interpolate the data occluded by the beam stop and we used Fourier weighted projections [31] on the pixels with values less than zero after background subtraction. Ten reconstructions from random starting guesses were registered and averaged. The individual reconstructions exhibited a small amount of defocusing so the registration procedure also included optimizing over a defocus term. After averaging the best focus position was set for the optimal contrast of the nanoparticles.

II. ACKNOWLEDGEMENT

III. AUTHOR CONTRIBUTIONS

M.G., J.R.F. and D.Z. conceived the sample design. D.Z., B.W., N.F. and K.O prepared the samples. D.Z., M.G., B.W., A.S. performed the coherent diffraction experiment. M.G. processed the data. Y.A., T.T. and P.F. performed the TXM and STXM measurements. A.S., M.F., J.R.F., and J.S. supervised the project. D.Z. prepared the manuscripts with contribution from all authors.

---

[1] SLAC Linac Coherent Light Source, http://lcls.slac.stanford.edu, (2009).

[2] FLASH, http://hasylab.desy.de/facilities/flash/index_eng.html (2009).

[3] J. Miao, P. Charalambous, J. Kirz, and D. Sayre, "Extending the methodology of x-ray crystallography to allow imaging of micrometre-sized non-crystalline specimens," Nature 400, 342 (1999).

[4] H. N. Chapman, A. Barty, M. Bogan, S. Boutet, M. Frank, S. P. Hau-Riege, S. Marchesini, B. W. Woods, W. H. B. S. Bajt, R. A. London, E. Plönjes, M. Kuhlmann, R. Treusch, S. Düsterer, T. Tschentscher, J. R. Schneider, E. Spiller, T. Möller, C. Bostedt, M. Hoener, D. A. Shapiro, K. O. Hodgson, D. van der Spoel, F. Burmeister, M. Bergh, C. Caleman, G. Huldt, M. M. Seibert, F. R. N. C. Maia, R. W. Lee, A. Szöke, N. Timneanu, and J. Hajdu, "Femtosecond diffractive imaging with a soft-x-ray free-electron laser," Nat. Physics 2, 839 (2006).

[5] A. Barty, S. Boutet, M. J. Bogan, S. P. Hau-Riege, S. Marchesini, K. Sokolowski-Tinten, N. Stojanovic, R. Tobey, H. Ehrke, A. Cavalleri, S. Düsterer, S. Bajt, B. Woods, M. M. Seibert, J. Hajdu, R. Treusch, and H. N. Chapman, "Ultrafast single-shot diffraction imaging of nanoscale dynamics," Nat. Photonics 2, 415 (2008).

[6] A. Ravasio, D. Gauthier, F. R. N. C. Maia, M. Billon, J.-P. Caumes, M. G. D. Garzella, O. Gobert, J.-F. Hergott, A.-M. Pena, H. Perez, B. Carrea, E. Bourhis, J. Gierak, A. Madouri, D. Mailly, B. Schiedt, M. Fajardo, J. Gautier, P. Zeitoun, P. H. Bucksbaum, J. Hajdu, , and H. Merdji, "Single-shot diffractive imaging with a table-top femtosecond soft x-ray laser-harmonics source," Phys. Rev. Lett. 103, 028104 (2009).

[7] R. Mitzner, M. Need, T. Noll, N. Pontius, and W. Eberhardt, "An x-ray autocorrelator and delay line for the VUV-FEL at TTF/DESY," Proc. of SPIE 59200D (2005).

[8] W. Roseker, H. Franz, H. Schulte-Schrepping, A. Ehnes, O. Leupold, F. Zontone, A. Robert, and G. Grübel, "Performance of a picosecond x-ray delay line unit at 8.39 kev," Opt. Lett. 34, 1768 (2009).

[9] M. Guizar-Sicairos and J. R. Fienup, "Holography with extended reference by autocorrelation linear differential operation," Opt. Express 15, 17592 (2007).

[10] I. McNulty, J. Kirz, C. Jacobsen, E. D. Anderson, M. R. Howells, and D. P. Kern, "High resolution imaging by fourier transform x-ray holography," Science 256, 1009 (1992).

[11] S. Eisebitt, J. Lüning, W. F. Schlotter, M. Lörgen, O. Hellwig, W. Eberhardt, and J. Stöhr, "Lensless imaging of magnetic nanostructures by x-ray spectro-holography," Nature 432, 885

(2004).

[12] S. G. Podoro, K. M. Pavlov, and D. M. Paganin, "A non-iterative reconstruction method for direct and unambiguous coherent diffractive imaging," Opt. Express **15**, 9954 (2007).

[13] S. Marchesini, S. Boutet, A. E. Sakdinawat, M. J. Bogan, S. Bajt, A. Barty, H. N. Chapman, M. Frank, S. P. Hau-Riege, A. Szöke, C. Cui, D. A. Shapiro, M. R. Howells, J. C. H. Spence, J. W. Shaevitz, J. Y. Lee, J. Hajdu, and M. M. Seibert, "Massively parallel x-ray holography," Nat. Photonics **2**, 560 (2008).

[14] M. Guizar-Sicairos and J. R. Fienup, "Direct imaging reconstruction from a fourier intensity pattern using heraldo," Opt. Lett. **33**, 2668 (2008).

[15] M. Guizar-Sicairos, D. Zhu, J. R. Fienup, B. Wu, A. Scherz, and J. Stöhr, "Holographic x-ray imaging reconstruction through the application of differential and integral operators," submitted.

[16] D. L. Fried, "Least-square fitting a wave-front distortion estimate to an array of phase-difference measurements," J. Opt. Soc. Am **67**, 370 (1977).

[17] R. H. Hudgin, "Wave-front reconstruction for compensated imaging," J. Opt. Soc. Am. **67**, 375 (1977).

[18] W. H. Southwell, "Wave-front estimation from wave-front slope measurement," J. Opt. Soc. Am. **70**, 998 (1980).

[19] A. Shavel, B. Rodríguez-González, M. Spasova, M. Farle, and L. M. Liz-Marzán, "Synthesis and characterization of iron/iron oxide core/shell nanocubes," Adv. Funct. Mater. **17**, 3870 (2007).

[20] L. P. Yaroslavsky and H. J. Caulfield, "Deconvolution of multiple images of the same object," Appl. Opt. **33**, 2157 (2007).

[21] J. R. Fienup, "Phase retrieval algorithms: a comparison," Appl. Opt. **21**, 2758–2769 (1982).

[22] H. N. Chapman, A. Barty, S. Marchesini, A. Noy, S. P. Hau-Riege, M. R. H. C. Cui, R. Rosen, H. He, J. C. H. Spence, U. Weierstall, and D. S. T. Beetz, C. Jacobsen, "High-resolution ab initio three-dimensional x-ray diffraction microscopy," J. Opt. Soc. Am. A **23**, 1179 (2006).

[23] R. L. Sandberg, D. A. Raymondson, C. L. o vorakiat, A. Paul, K. S. Raines, J. Miao, M. M. Murnane, H. C. Kapteyn, and W. F. Schlotter, "Tabletop soft-x-ray fourier transform holography with 50 nm resolution," Opt. Lett. **34**, 1618 (2009).

[24] W. F. Schlotter, R. Rick, K. Chen, A. Scherz, J. Stöhr, J. Lüning, S. Eisebitt, C. Günther,

W. Eberhardt, O. Hellwig, and I. McNulty, "Multiple reference fourier transform holography with soft x-rays," Appl. Phys. Lett. **89**, 163112 (2006).

[25] W. Chao, B. D. Harteneck, J. A. Liddle, E. H. Anderson, and D. T. Attwood, "Soft x-ray microscopy at a spatial resolution better than 15 nm," Nature **435**, 1210 (2005).

[26] W. Chao, J. Kim, S. Rekawa, P. Fischer, and E. H. Anderson, "Demonstration of 12 nm resolution fresnel zone plate lens based soft x-ray microscopy," Opt. Express **17**, 17669 (2009).

[27] M. J. Bogan, W. H. Benner, S. Boutet, U. Rohner, M. Frank, A. Barty, M. M. Seibert, F. Maia, S. Marchesini, S. Bajt, B. Woods, V. Riot, S. P. Hau-Riege, M. Svenda, E. Marklund, E. Spiller, J. Hajdu, and H. N. Chapman, "Single particle x-ray diffractive imaging," Nano Lett. **8**, 310 (2008).

[28] A. Scherz, W. Schlotter, K. Chen, R. Rick, J. Stöhr, J. Lüning, I. McNulty, C. Günther, F. Radu, W. Eberhardt, O. Hellwig, and S. Eisebitt, "Phase imaging of magnetic nanostructures using resonant soft x-ray holography," Phys. Rev. B **76**, 214410 (2007).

[29] S. T. Thurman and J. R. Fienup, "Phase-error correction in digital holography," J. Opt. Soc. Am. A **25**, 983 (2008).

[30] J. R. Fienup, "Lensless coherent imaging by phase retrieval with an illumination pattern constraint," Opt. Express **14**, 498 (2006).

[31] M. Guizar-Sicairos and J. R. Fienup, "Phase retrieval with fourier-weighted projections," J. Opt. Soc. Am. A **25**, 701 (2008).
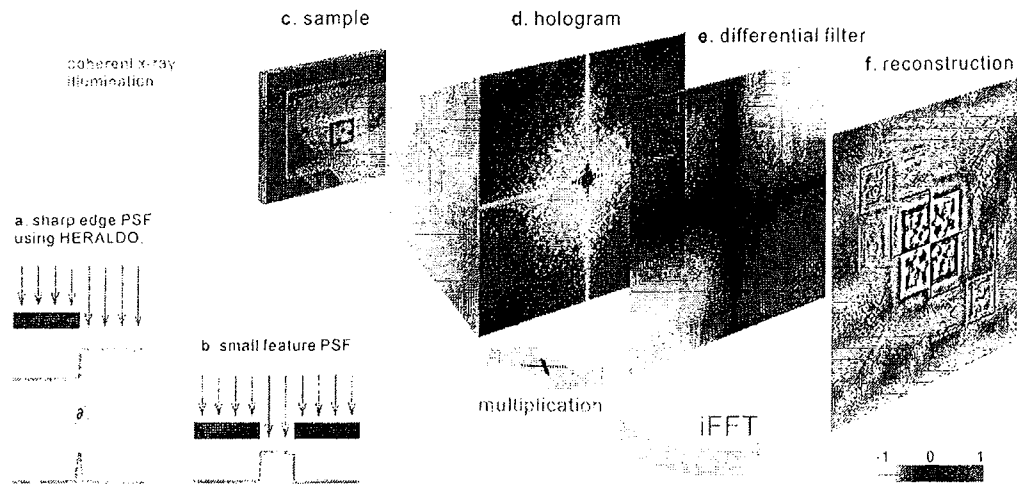
FIG. 1: **HERALDO schematics.** a and b, illustration comparing the point spread function (PSF) from a sharp edge after differential operation and the PSF from a small feature, e.g. a reference hole. c. The object and reference structures are illuminated with a coherent X-ray beam. d. The incident beam is scattered by both the object and the references and a hologram is recorded by a 2-D array detector in the far field; intensity shown here in log scale. e. Linear differential filter is multiplied with the diffraction intensity. f A single Fourier transform delivers three relief images of the "cheese" from which the final reconstruction is computed.
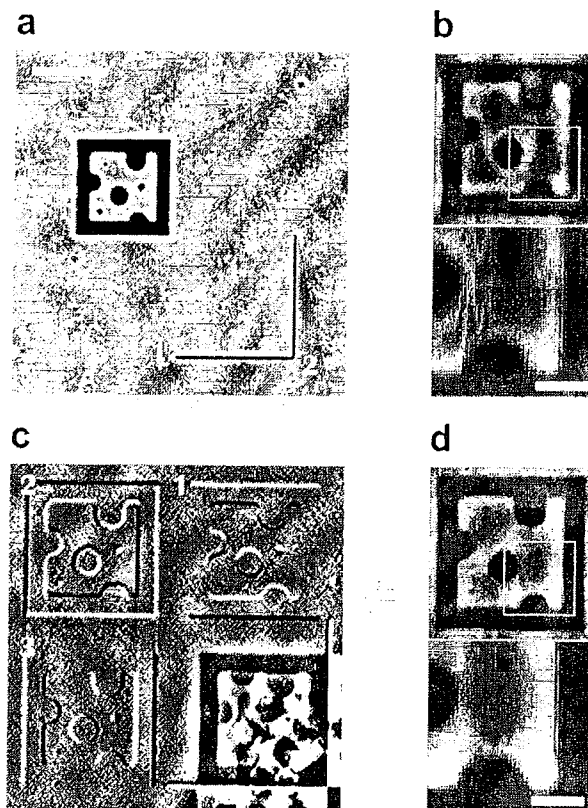
FIG. 2: "Cheese" sample reconstructions. a. SEM overview of the "cheese" object and the reference structures; scale bar is 1 μm. b. FTH reconstruction and the magnified view of the lower right corner, with 200 nm scale bar. c. the three relief images obtained. d. HERALDO reconstruction from c and the magnified view of the lower right corner, with 200 nm scale bar.
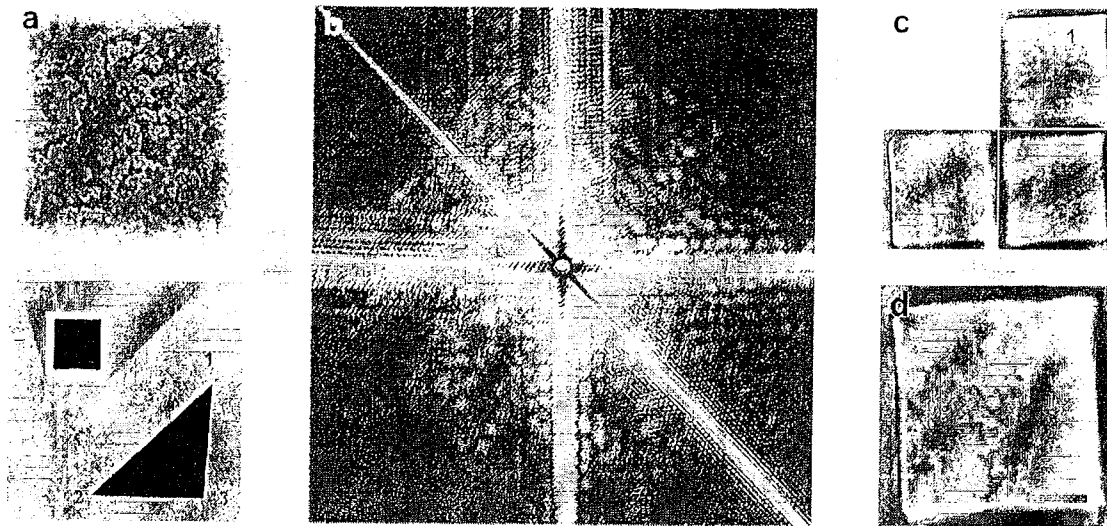
FIG. 3: **Nanocube reconstruction.** a. SEM images of the sample: nanocubes within the square aperture supported by Si_3Ni_4 (upper) and the gold side overview where one can also see the triangular reference (lower). b. Measured diffraction intensity in log scale. c. individual images obtained from the the three corners are combined to obtain the final reconstruction in d. Scale bar corresponds to 300 nm.
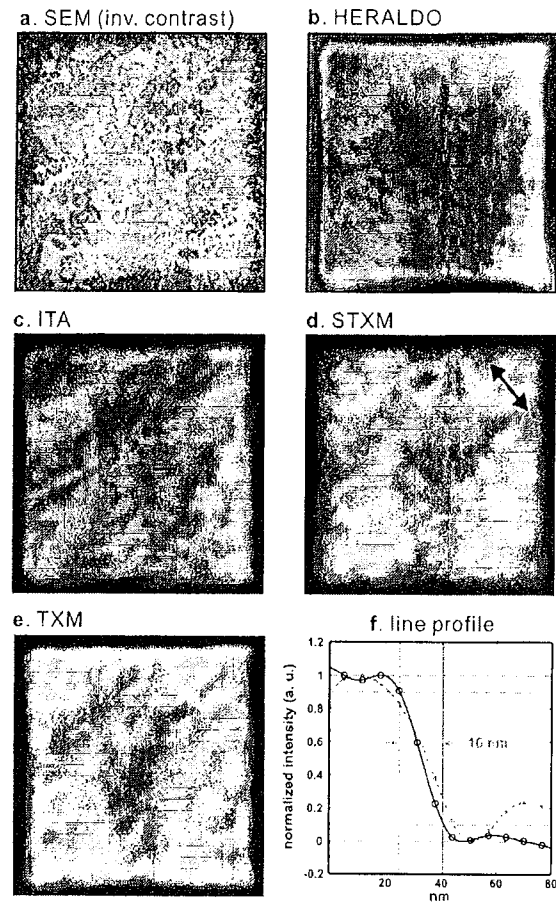
a. SEM (inv. contrast) b. HERALDO
c. ITA d. STXM
e. TXM f. line profile

FIG. 4: **Comparison of different methods.** a. SEM image with the contrast inverted for easier comparison. b. HERALDO reconstruction, c. ITA result. d. STXM image obtained with 20 nm zone plate; scanning direction marked by arrow. e. TXM image obtained with 25 nm objective zone plate. f. comparison of line cut profile as indicated in b. for HERALDO (circles, solid line fitting) and c. for ITA (crosses, dashed fitting). For this line cut, the HERALDO reconstruction gives 16 nm resolution according to the 10-90% criterion compared with 24 nm for ITA.